


Cite this: *RSC Adv.*, 2024, **14**, 24712

# Smart hydrogel composite for microenvironmental humidity regulation in cigar storage

Xiaoying Ji,<sup>a</sup> Xiaopeng Li,<sup>a</sup> Juan Liu,<sup>a</sup> Di Wu,<sup>b</sup> Qianqian Liang,<sup>b</sup> Beibei Zhu,<sup>a</sup> Wanjiao Fang,<sup>a</sup> Shirui Qiu,<sup>a</sup> Qianying Zhang,<sup>\*a</sup> Dongliang Li,<sup>\*a</sup> Lijuan Zhao<sup>b</sup> and Yi Wang<sup>ID<sup>b</sup></sup>

Environmental humidity profoundly influences various life activities, especially for plants that depend heavily on optimal humidity for growth. The humidity index is particularly crucial for preserving the functionality of plant leaves, notably in economically valuable plants such as cigar tobacco. This paper introduces a novel dual-layer moisturizing material, a PAS-PDMS composite, based on polyacrylamide/solketal (PAS) hydrogel and polydimethylsiloxane (PDMS). This material features a unique hierarchical water release mechanism. Comprehensive analyses, including thermogravimetric analysis, Fourier-transform infrared spectroscopy, low-field nuclear magnetic resonance, and dynamic water adsorption studies, confirm the water migration and humidity control mechanisms of the PAS-PDMS composite. This smart hydrogel composite regulates microenvironmental humidity bidirectionally. When applied to cigar boxes for storage, it stabilizes internal humidity at approximately 65%, maintaining this level for over 20 days. Furthermore, the PAS-PDMS composite exhibits superior mechanical properties and light transmittance, achieving an exceptional transmittance of 84%. In conclusion, the PAS-PDMS composite offers intelligent humidity control, providing a novel approach to the storage and preservation of cigars.

Received 8th April 2024

Accepted 31st July 2024

DOI: 10.1039/d4ra02622e

rsc.li/rsc-advances

## 1. Introduction

Cigars hold the undisputed position as the “kings” of the tobacco industry,<sup>1</sup> renowned for their rich and mellow smoke alongside their exquisite taste. Throughout their history, cigars have played a pivotal role, consistently gaining market share year after year. However, the taste and value of cigars<sup>2</sup> hinge significantly on the “curing” process during storage. Many cigar aficionados currently advocate for maintaining cigars at an ideal storage humidity of 68–72%. Within the precise humidity range, cigars flourish, maturing gracefully and burning evenly, thereby greatly enhancing the experience for avid cigar enthusiasts. As a globally cherished tobacco product, cigars have not only promoted economic development but also elevated people’s sense of well-being. With the rise in living standards, the demand for cigars has soared, accompanied by an increasingly refined pursuit of flavor. Advances in science and technology have revolutionized the seamless and swift global circulation of cigars, allowing individuals worldwide to savor cigars from diverse origins. However, the preservation of cigars requires stringent humidity control, presenting significant challenges during long-distance

transportation. Therefore, maintaining optimal humidity conditions throughout the journey is crucial to safeguarding the authenticity and quality of these prized smokes. Conversely, excessive humidity leads to damp cigars that are difficult to ignite and prone to mold growth.<sup>3</sup> Both overly dry and overly humid environments can negatively impact cigar quality, even leading to damage. Therefore, it is imperative to develop methods to maintain appropriate humidity levels in cigar storage environments. The predominant method for cigar storage involves using a constant temperature and humidity cabinet, but its limited portability and high economic and practical requirements present challenges. Consequently, there is a pressing need to develop a simple, portable material with excellent humidity regulation effects, addressing a critical issue for both cigar smokers and tobacco companies.

Recently, hydrogels,<sup>4</sup> which are functional polymer materials characterized by a three-dimensional network structure,<sup>5</sup> have gained prominence, particularly owing to their distinctive biocompatibility.<sup>6,7</sup> Widely employed in biomedicine,<sup>8–10</sup> flexible wearable devices,<sup>11</sup> and various applications involving the exchange of water molecules,<sup>12</sup> hydrogels face challenges owing to their susceptibility to drying and water loss,<sup>13</sup> ultimately compromising their ability to regulate water molecules.<sup>14</sup> The consequential shrinkage affects the original functions of the hydrogels,<sup>15</sup> necessitating measures to enhance their resistance to drying.<sup>16</sup> Current approaches typically involve<sup>17</sup> the addition of inorganic salts or organic phases,<sup>18</sup> which either increase the

<sup>a</sup>Cigar Fermentation Technology Key Laboratory of China Tobacco, Industrial Efficient Utilization of Domestic Cigar Tobacco Key Laboratory of Sichuan Province, China Tobacco Sichuan Industrial Co., Ltd., Chengdu 610066, China. E-mail: qianyingzhang@163.com

<sup>b</sup>College of Chemistry and Materials Science, Sichuan Normal University, Chengdu 610068, China



saturated vapor pressure of free water or introduce hydrogen bond<sup>19</sup> interactions to improve water retention.<sup>20</sup> However, the introduction of fillers can impact the mechanical properties of hydrogels.<sup>21</sup> To address this, there is a pressing need to design innovative hydrogel materials with intelligent humidity control capabilities. This would enhance the water retention capacity of hydrogels, enabling the intelligent control of water molecules.<sup>22</sup>

Building upon the aforementioned analysis, this study leverages polyacrylamide (PAM) hydrogel as its foundation,<sup>23</sup> integrating the humidity-regulating agent Solketal (Sol) and introducing free hydroxyl groups to instill a hydrogen-bond-based water-locking effect. Taking inspiration from the functions of the skin, we employ the hydrolysis of a silane coupling agent to introduce the organic silicon skin layer PDMS, resulting in a robust and adhesive composite material.<sup>24</sup> This unique structural design substantially amplifies the water retention capabilities of the hydrogel, enabling the precise control and release of water molecules. Consequently, the hydrogel can absorb water to reduce humidity in high-humidity environments and release water to elevate humidity in low-humidity environments.<sup>25</sup> Thus, it can effectively regulate humidity smartly and efficiently. Applying this material to the microenvironment of wooden cigar storage boxes, we scrutinize its moisture migration and evolution mechanisms. Our objective is to establish the most suitable microenvironment humidity for cigar storage, introducing a novel application method and technical approach for the tobacco industry (Scheme 1).

## 2. Results and discussion

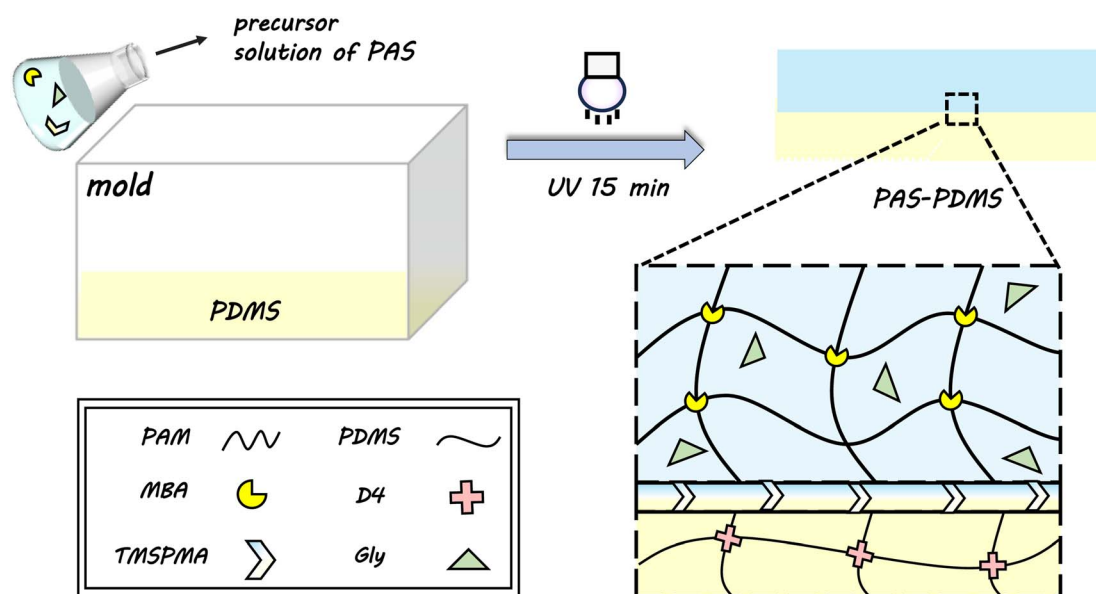
### 2.1 Molecular design and structural characterization of PAS-PDMS composite

Initially, the cross-section morphology of the PAS-PDMS composite was observed using a scanning electron microscope.<sup>16</sup>

As depicted in Fig. 1a–c, the PAS-PDMS composite possessed a distinctive double-layer structure,<sup>17</sup> with tightly integrated upper and lower layers. Elemental analysis revealed an even and complete distribution of elements such as C and N on the surface, indicating a lack of holes or defects.<sup>18</sup> Notably, the distribution of Si atoms was segregated (Fig. 1d), as they were concentrated entirely in the PDMS elastomer of the lower layer.<sup>19</sup> This skin-like design facilitates the controlled release and absorption of water molecules, effectively achieving the objective of intelligently adjusting the microenvironmental humidity balance.

Subsequently, the molecular structure of the material was characterized through infrared spectroscopy.<sup>20</sup> The results are depicted in Fig. 1(e). Two characteristic peaks are evident in the infrared spectrum of the PAS-PDMS composite at wavelengths of 1654 and 3650  $\text{cm}^{-1}$ . These peaks correspond to the characteristic stretching vibrations of the carbonyl ( $\text{C}=\text{O}$ ) and amino ( $\text{NH}_2$ ) groups within the acrylamide group,<sup>21</sup> respectively. Notably, no deviation is observed between the new peaks and the characteristic peaks of PAS hydrogel and PDMS elastomer.<sup>22</sup> This indicates that the PAS-PDMS composite, prepared using a silane coupling agent, did not include any new substances. Instead, the materials were bonded together through the robust interaction of hydroxyl groups generated by the hydrolysis of the silane coupling agent, maintaining strong adhesion without blocking the water control channels, thereby enhancing the humidity-regulating effect.<sup>23</sup>

The introduction of PDMS elastomer did not considerably deteriorate the light transmittance of the hydrogel material.<sup>24</sup> We conducted a test on the light transmittance of the PAS-PDMS composite using a UV spectrophotometer, revealing that its light transmittance is approximately 84%, compared to the 86% and 85% light transmittances of the PAS hydrogel and PDMS elastomer (Fig. 1f), respectively. Thus, the composite double-layer material maintained a high light transmittance,<sup>25</sup>



Scheme 1 Network structure design of the PAS/PDMS composite.

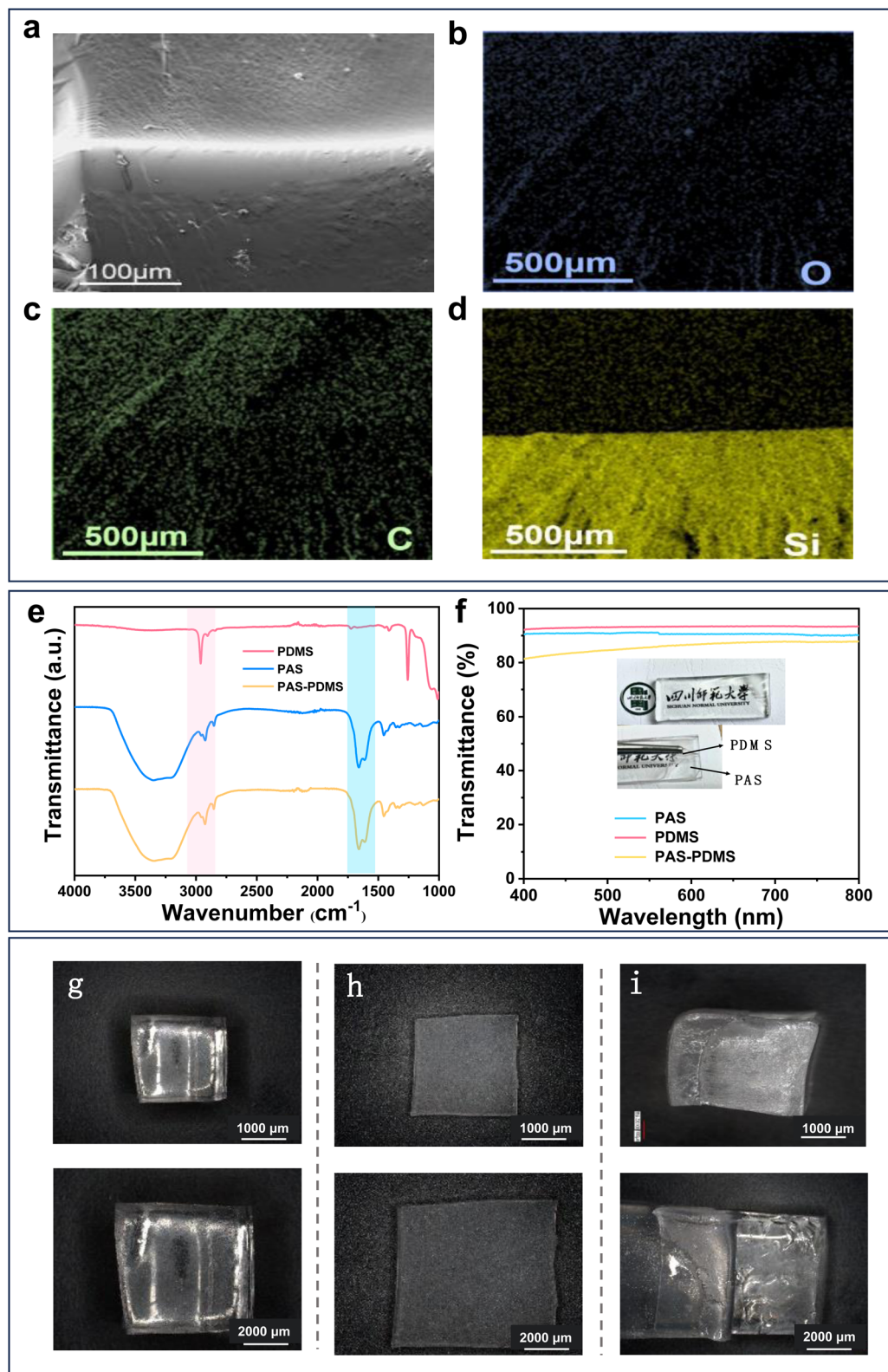


Fig. 1 Characterization of the PAS-PDMS composite: (a) SEM image, (b–d) EDS spectra, (e) infrared spectrum, and (f) UV spectrum; super depth field optical images of the (g) PAS hydrogel, (h) PDMS elastomer, and (i) PAS-PDMS composite.

meeting the visual requirements for cigar boxes. To further elucidate the bonding mechanism of the PAS-PDMS composite, we characterized its surface structure using an ultra-depth-of-

field optical microscope.<sup>26</sup> The results corresponding to the PAS hydrogel, PDMS elastomer, and PAS-PDMS composite are shown in Fig. 1(f)–(h), respectively. Note that the surfaces of





both the PAS hydrogel<sup>27</sup> and the PDMS elastomer are smooth, flat, and transparent. However, when the PAS-PDMS composite was peeled at a 180° angle and enlarged images were taken,<sup>28</sup> the surface of PDMS was rough and uneven owing to the hydrolysis of the silane coupling agent. This is similar to the hydrolysis of a riveted silane coupling agent(3-(trimethoxysilyl) propyl methacrylate).<sup>29</sup> The two phases of the PAS-PDMS composite are endowed with a strong bonding effect, ensuring structural stability during humidity regulation.<sup>30</sup>

## 2.2 Rheological property test of PAS-PDMS composite

The successful integration of high-strength PDMS elastomer significantly enhances the structural network strength of the PAS-PDMS composite. We conducted tests on the network structure and strength of the PAS-PDMS composite using a rotary rheometer, and the results are displayed in Fig. 2. Fig. 2(a)–(c) represent the frequency scans of PAS hydrogel, PDMS elastomer, and PAS-PDMS composite, respectively. The loss modulus ( $G'$ ) and storage modulus ( $G''$ ) of the PDMS elastomer are higher than those of the PAS hydrogel, attributed to the stronger chain stiffness and cross-linking density of the PDMS elastomer, which effectively transmitted this strength to the PAS-PDMS composite.  $G'$  and  $G''$  of the PAS-PDMS composite are significantly higher than those of both PAS hydrogel and PDMS elastomer. Subsequently, strain scanning on the three materials produced results consistent with the frequency scans (Fig. 2d–f). Notably,  $G'$  of the PAS-PDMS composite did not exhibit a significant decline under the strain scanning mode (Fig. 2g and h). This indicates that the water molecular humidity control channel we established did not collapse under large strain, maintaining the stable internal network strength of the material. In summary, we have successfully integrated PDMS elastomer into the hydrogel, creating a moisture-regulating skin layer that enhances the network stiffness of the PAS-PDMS composite, meeting the mechanical load requirements during cigar box transportation. Therefore, the development of a moisture-regulating skin layer within the composite was a notable achievement. This layer not only enhanced the network stiffness but also ensured that the composite could meet the mechanical load requirements during cigar box transportation, addressing a practical need in the industry. The rheological property tests confirmed that the integration of PDMS elastomer into the PAS hydrogel matrix significantly improved the mechanical properties of the composite. The PAS-PDMS composite demonstrated a stable and robust network capable of withstanding mechanical stresses, making it a suitable material for applications requiring both strength and elasticity.

## 2.3 Mechanical property tests

The mechanical properties of the PAS-PDMS composite, as depicted in Fig. 3, indicate its robustness and durability, making it suitable for humidity regulation applications.<sup>30</sup> The 180° peel test reveals a peak stress of approximately 20 kPa, with a corresponding strain of around 750%, indicating strong adhesion between the PAS hydrogel and the PDMS substrate

(Fig. 3a and b). The stress–strain histogram shows minimal variance in peak stress values across different samples, suggesting consistent adhesion properties (Fig. 3c). Furthermore, the ultimate tensile stress of the PAS-PDMS composite increased from 0.1 MPa to approximately 0.8 MPa after the introduction of PDMS, demonstrating the high ductility of the composite (Fig. 3d). This result indicates that the incorporation of PDMS elastomer significantly enhances the mechanical characteristics of the PAS-PDMS composite. Notably, the compression stress of the PAS-PDMS composite remained nearly constant over 500 cycles without separation (Fig. 3e), showcasing its resilience under repeated compressive loads. These performance metrics underline the PAS-PDMS composite's robustness and suitability for practical applications where mechanical durability is crucial, making it a promising material for humidity regulation in cigar storage and other similar applications. The significant enhancement in ultimate tensile stress and compression stress stability highlights the synergistic effect of combining PAS hydrogel with PDMS elastomer. The PDMS component provides structural integrity and elasticity, while the PAS hydrogel offers flexibility and water retention capabilities. This combination results in a composite material that not only meets but exceeds the mechanical requirements for humidity regulation applications, particularly in the storage of sensitive products like cigars. Moreover, the high ductility and strong adhesion properties of the PAS-PDMS composite suggest that it can effectively withstand the mechanical stresses encountered during the transportation and handling of cigar boxes. The strong adhesion between the layers ensures that the composite remains intact, preventing delamination and preserving its functionality.

## 2.4 Water migration and evolution mechanism of PAS-PDMS composite

The unique network hierarchy and skin-like structural design of the PAS-PDMS composite enable it to systematically release water molecules, allowing for stable and smart humidity regulation across varying humidity environments. To validate this hypothesis, we conducted a comprehensive analysis of the water migration and evolution mechanism of the PAS-PDMS composite. Initially, thermogravimetry-infrared (TGA-IR) analysis was employed to monitor the temperature-dependent release process of water and assess its thermal stability. The results, depicted in Fig. 4a–c, reveal three peaks in the 700–1200  $\text{cm}^{-1}$  wavenumber range at 500 °C, corresponding to the thermal cracking process of poly(dimethylsiloxane) and the breaking of Si–O bonds. This indicates that the introduction of the PDMS elastomer imparts high thermal stability to the material, with complete decomposition occurring at 500 °C. Notably, the broad peak detected at 3200–3400  $\text{cm}^{-1}$  from 25 to 150 °C corresponds to the vibration peak of water hydroxyl groups. As the temperature increased, the peak intensity of the water hydroxyl groups gradually rose, reaching its zenith at approximately 100 °C. It suggests progressive water release and optimal humidity regulation. Around 150 °C, the peak intensity decreased, indicating that the temperature for water release

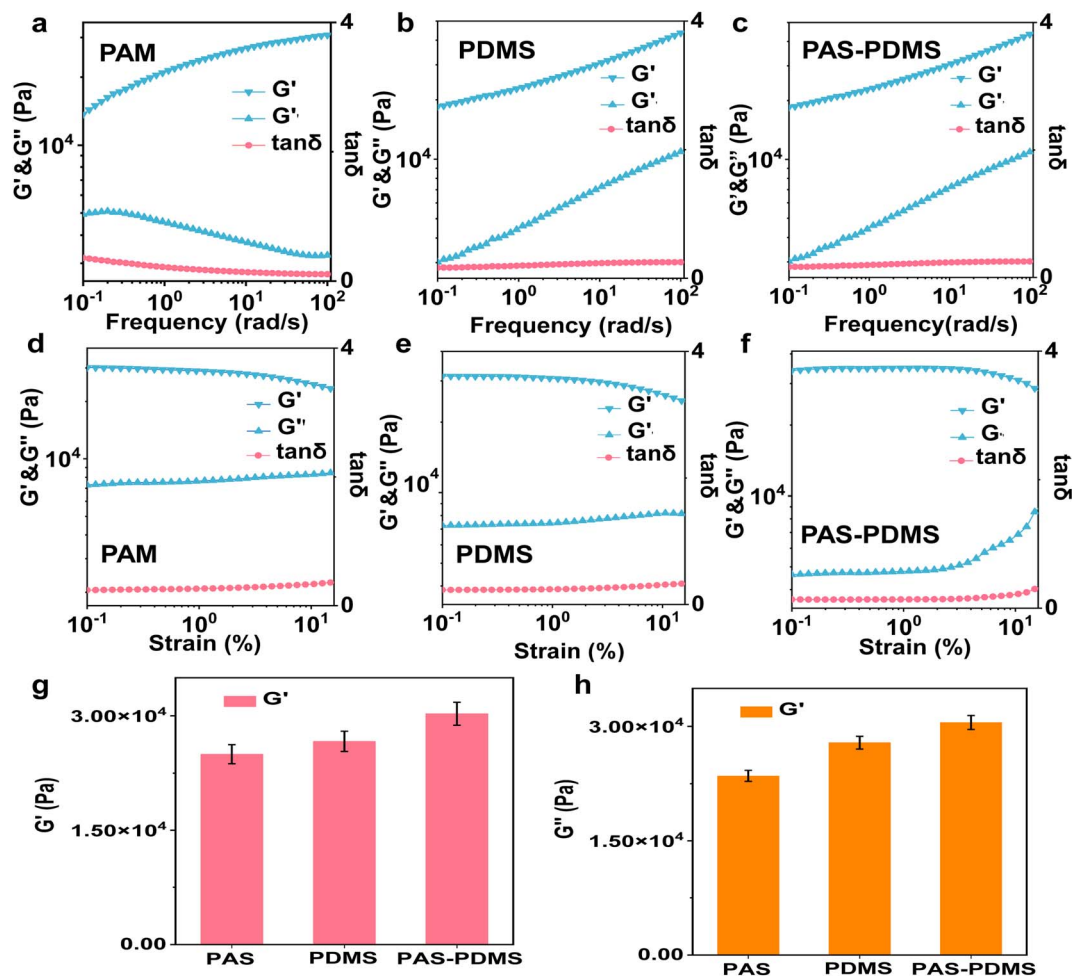


Fig. 2 Frequency scan rheological curves of the (a) PAS hydrogel, (b) PDMS elastomer, (c) PAS-PDMS composite; strain scan rheological curves of the (d) PAS hydrogel, (e) PDMS elastomer, (f) PAS-PDMS composite; (g) comparative frequency scan modulus of the three materials; (h) comparative frequency strain modulus of the three materials.

exceeded the vaporization temperature of water ( $100\text{ }^{\circ}\text{C}$ ). This implies that the PAS-PDMS composite exhibited superior water release characteristics at elevated temperatures, which is critical for sustained humidity control.

A two-dimensional mapping image of the entire water release process illustrated that the temperature range for water release in the PAS-PDMS composite was between  $50$  and  $150\text{ }^{\circ}\text{C}$ . Beyond  $150\text{ }^{\circ}\text{C}$ , the blue area decreases by half, indicating the complete and gradual release of water. This composite structure, with its skin protection, significantly enhanced the humidity regulation efficiency of the material, meeting the requirements for extended cigar storage. The differential thermogravimetric (DTG) curve of the PAS-PDMS composite, shown in Fig. 4(d), displayed a sharp peak from  $25$  to  $180\text{ }^{\circ}\text{C}$ , corresponding to the weight loss process due to stepwise water release within this temperature range. The thermodynamic parameters of the PAS-PDMS composite, presented in Fig. 4(e), revealed that PAS hydrogel exhibited a wide peak at  $-20\text{ }^{\circ}\text{C}$ , corresponding to the crystallization peak of water molecules in the system. However, with the introduction of PDMS elastomer, the PAS-PDMS composite did not exhibit a crystallization peak,

suggesting enhanced anti-freezing capabilities and stable microenvironment regulation even under extreme low-temperature conditions.

To delve into the microscopic mechanism of water release and the state of water molecules within the PAS-PDMS composite system, we conducted low-field NMR tests. Fig. 5(a) and (b) presented the results, showcasing two distinct peaks during the relaxation time of  $0.1$ – $10\text{ ms}$ , representing two different forms of bound water in the PAS-PDMS composite system: strongly and weakly bound water. The introduction of the hydroxyl group of acetone glycidyl fostered hydrogen bonding with water in the PAS-PDMS composite system, resulting in a certain degree of water locking that surpassed the weak water bonding formed by the hydrogel itself. As relaxation time increased, another peak emerged in the range of  $100$ – $1000\text{ ms}$ , corresponding to free water in the hydrogel system. Measurements of the moisture content at three bonding degrees indicated a gradual increase in moisture content with decreasing bonding degree. Essentially, the PAS-PDMS composite maintained the highest free water content while concurrently retaining two types of bound water. This



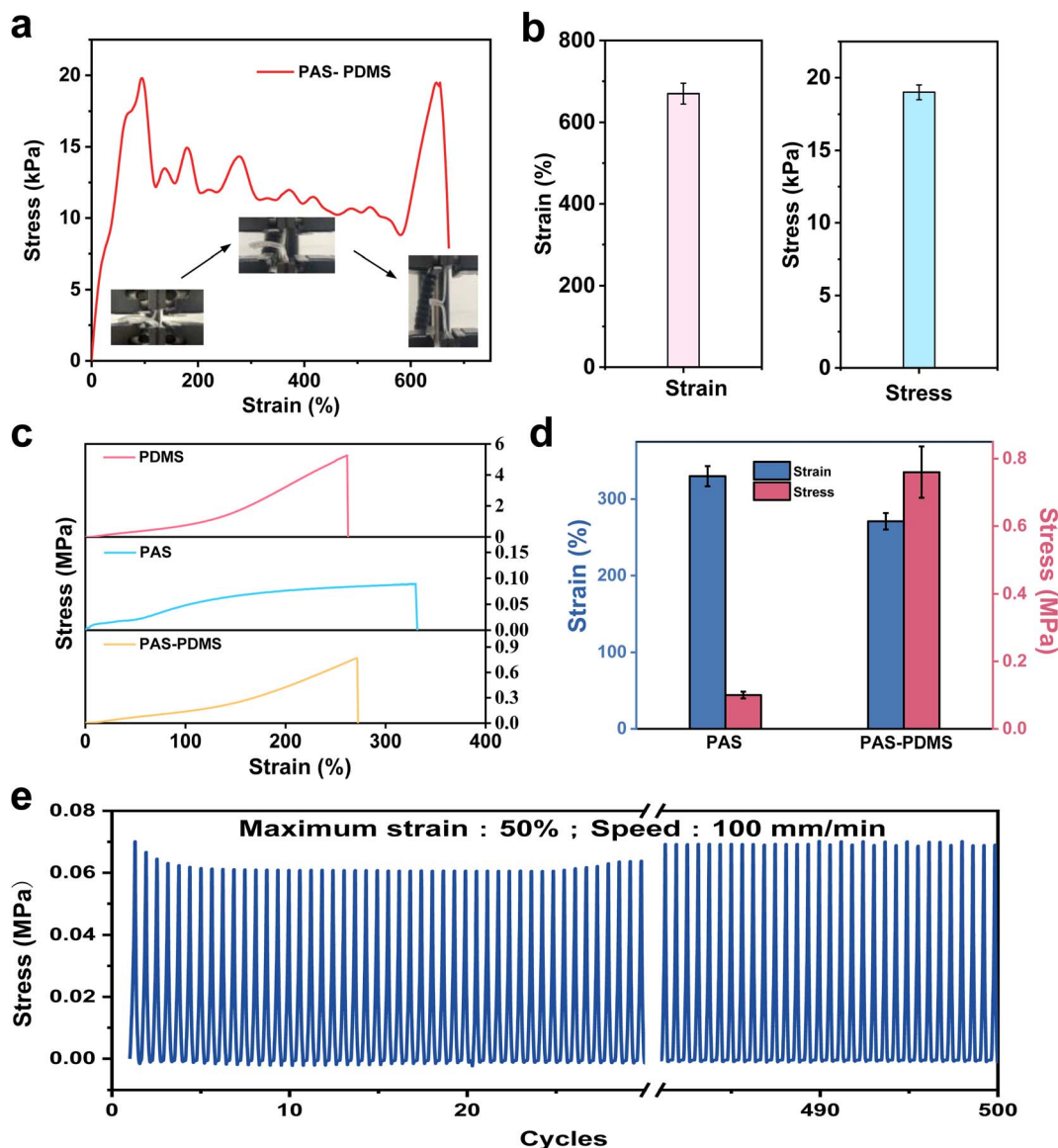


Fig. 3 PAS-PDMS composite's (a) stress-strain curve of 180° peel test, (b) stress-strain histogram of 180° peel test, (c) stress-strain curve of the uniaxial tensile test at break, (d) stress-strain histogram of the uniaxial tensile test at break, (e) stress-cycle compression curve.

distinctive water-binding mechanism empowered the PAS-PDMS composite to release water gradually, optimizing humidity regulation efficiency and meeting the requirements for regulating humidity in extreme environments.

To demonstrate the intelligent humidity control capability of the PAS-PDMS composite, we conducted water adsorption kinetics tests, as illustrated in Fig. 5(c) and (d). The hydrogel promptly absorbed water, achieving a sample mass growth rate of 45% within 10 hours. As environmental humidity decreased, the rate of hydrogel weight change gradually diminished, indicating its ability to sense and respond to external humidity changes by releasing water. Notably, when environmental humidity fell below 40%, the quality change rate of the hydrogel became negative, signifying its capability to release absorbed water for microenvironmental humidity adjustment and diffuse water to the external environment, enhancing humidity in

extremely dry conditions. The adsorption isotherm confirmed roughly equal water absorption and release qualities at this stage, highlighting the sustained humidity control performance of the material without dehydration-induced loss. As external humidity gradually increased to 95%, the quality change rate of the hydrogel rose, while the total water absorption capacity remained consistent, demonstrating excellent repeated humidity control performance (Fig. 5e). The adsorption isotherm revealed consistent relative mass change rates, indicating stable cycling between water absorption and release under high- and low-humidity conditions, respectively. Furthermore, the presence of strongly bound water in the system (Fig. 5f) ensured that the material did not completely release all water, retaining the ability to further regulate humidity. The rapid sensing and intelligent control capabilities of the PAS-PDMS composite across a wide range of humidity

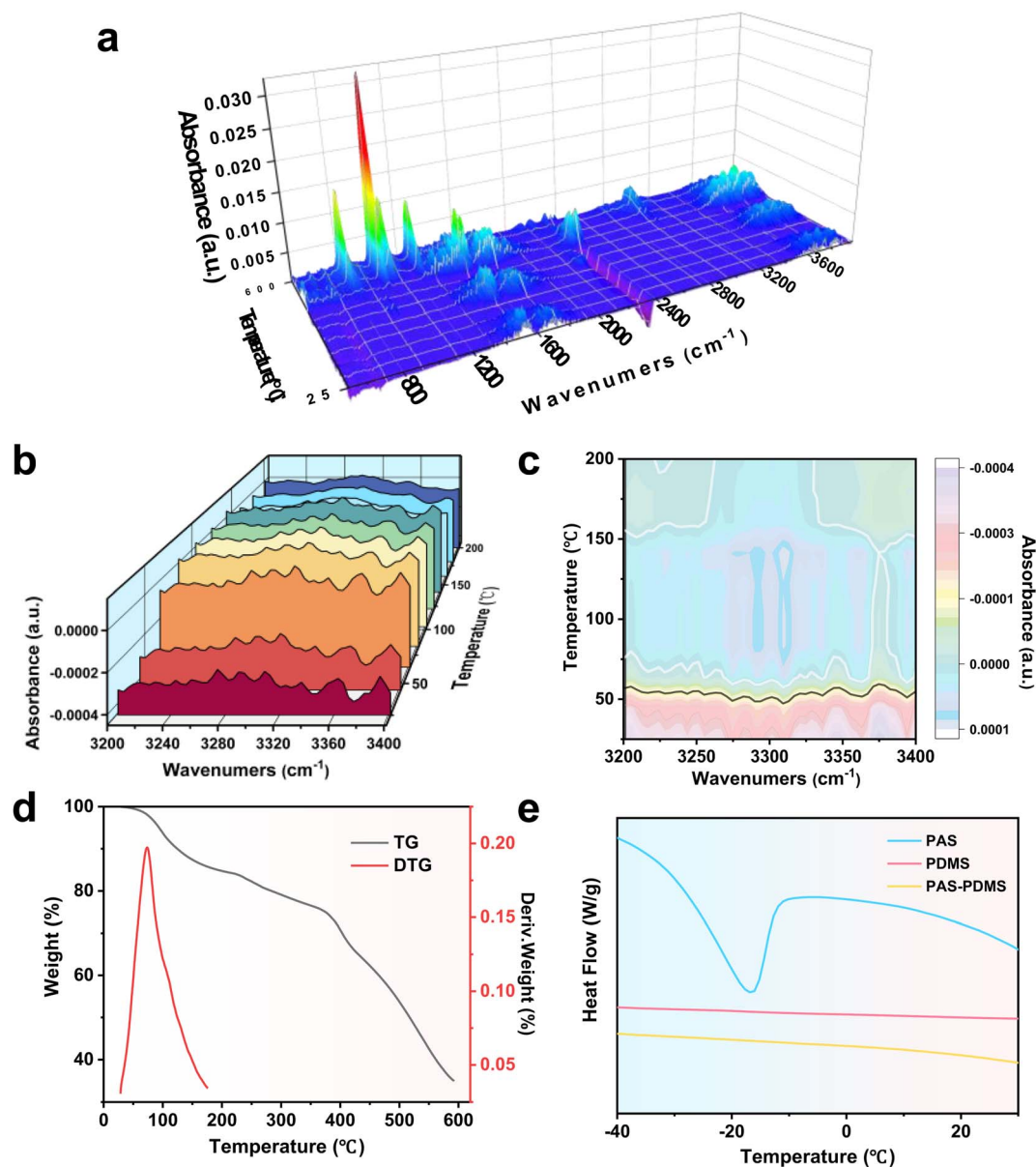


Fig. 4 The PAS-PDMS composite's (a) TG-IR 3D map, (b) TG-IR water peak hydroxyl waterfall map, (c) TG-IR 2D color map, (d) TG-IR thermogravimetric curve of the PAS-PDMS composite, and (e) differential scanning temperature enthalpy curves of the PAM hydrogel, PDMS elastomer, and PAS-PDMS composite.

conditions established its suitability for application in cigar box microenvironments.

Finally, we assessed the water retention capacity of the PAS-PDMS composite through weighing, revealing a mass retention rate of 94% within 12 h, significantly surpassing the 45% mass retention rate of PAS hydrogel without the skin layer protection (Fig. 5g and h). The introduction of PDMS elastomer not only conferred smart humidity control but also substantially enhanced the timeliness of this control ability, meeting the prolonged storage requirements of cigars. The enhanced retention capability ensures the material's effectiveness over extended periods, which is critical for maintaining the quality of stored cigars.

## 2.5 Humidity control performance test

To evaluate the humidity control performance of the PAS-PDMS composite, we positioned it at the base of a cigar box, covered by a hollow inner box to isolate the cigars from the hydrogel without affecting its humidity control capabilities. We placed a hygrometer and cigars within the hollow box (Fig. 6a) and conducted experiments with humidity levels set at 30%, 60%, and 90%. A blank group was also established for comparison. Our results demonstrated that the PAS-PDMS composite consistently maintained effective humidity control across diverse environments. In particular, the hydrogel exhibited stable regulation of water and humidity in the room-temperature setting (Fig. 6b). In the constant-temperature and





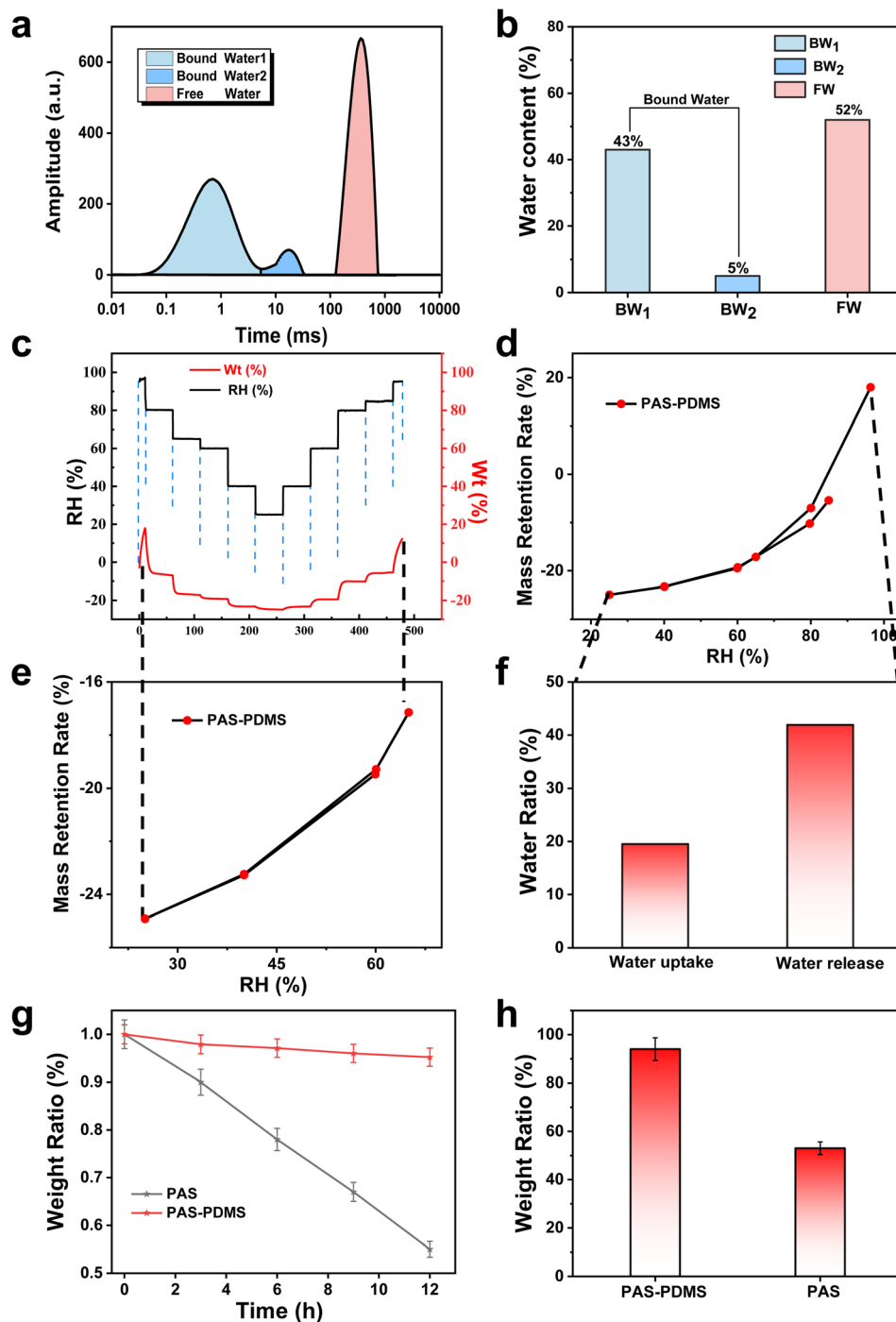
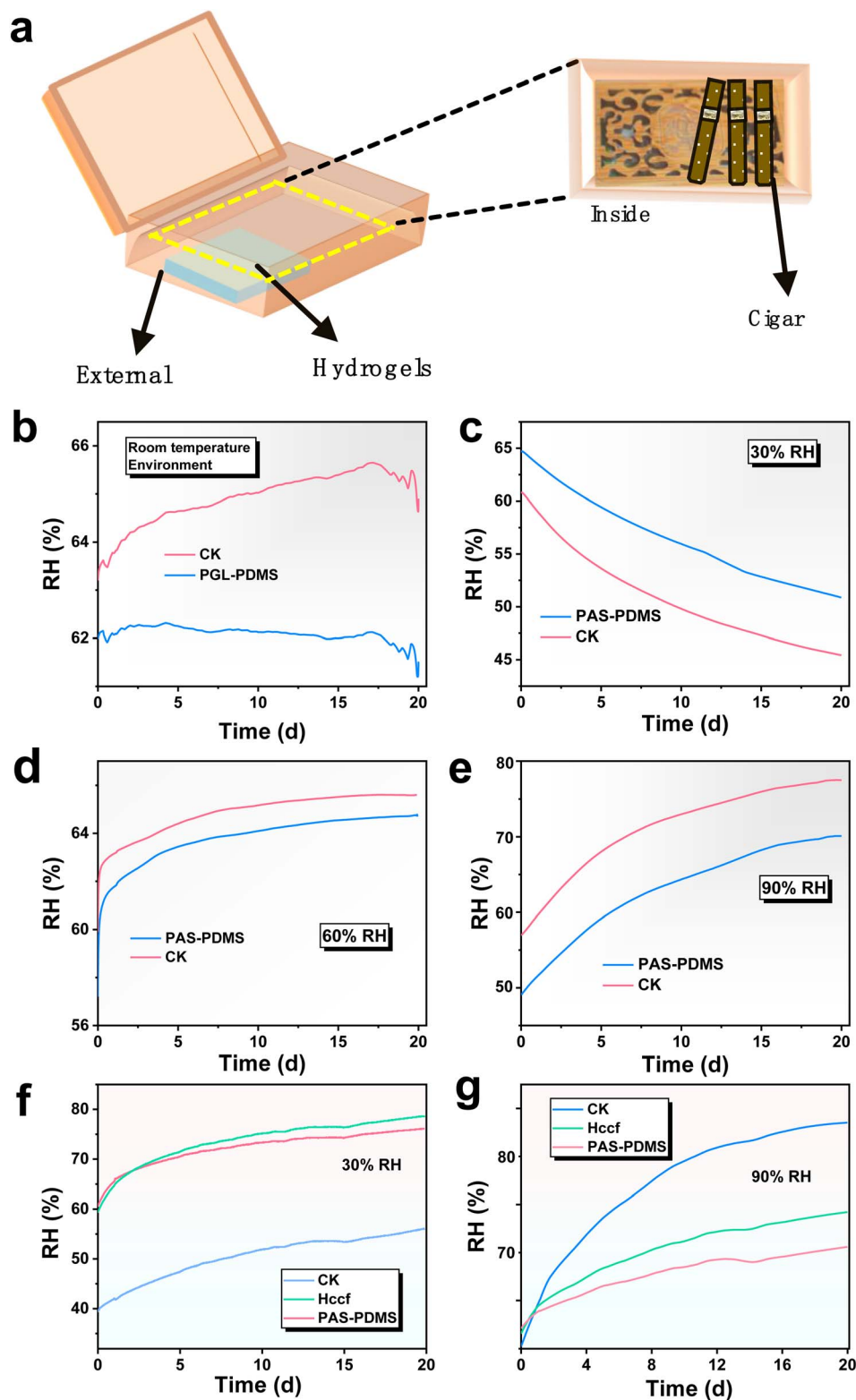


Fig. 5 The PAS-PDMS composite's (a) low field nuclear magnetic resonance spectrum, (b) low field nuclear magnetic resonance water peak area, (c) water adsorption kinetics curve, (d) water adsorption kinetics adsorption isotherm, (e) adsorption isotherm corresponding to "negative mass retention rate", (f) mass change histogram corresponding to water absorption gain and water release loss, (g) water retention curve of the PAS-PDMS composite and PAS hydrogel, (h) weight loss histogram corresponding to water retention curve.

-humidity box, the final humidity control outcomes in the low, medium, and high humidity environments were 52%, 65%, and 70%, respectively (Fig. 6c–e). These values fell within the optimal humidity range for cigars and persisted for up to 20 days, ensuring the quality of the cigars while providing long-term stability.

In addition, we conducted a comparative analysis between our prepared hydrogel materials and commercially available hydrogel-based moisturizing materials. The commercial hydrogels demonstrated some humidity control capability in both high- and low-humidity environments (Fig. 6f and g), but their performance was less effective compared to the PAS-PDMS





**Fig. 6** (a) Diagram of the PAS-PDMS composite for cigar humidity control. The PAS-PDMS composite's (b) room temperature humidity control curve, (c) 30% RH humidity control curve, (d) 60% RH humidity control curve, (e) 90% RH humidity control curve, (f) comparison of humidity control performance with Hccf under 30% RH conditions, and (g) comparison of humidity control performance with Hccf under 90% RH conditions.



composite. Moreover, they exhibited slower response speeds. The PAS-PDMS composite, on the other hand, employed a more agile and smarter humidity control strategy, swiftly maintaining the microenvironment's humidity within the optimal storage range for cigars. This ensures comprehensive protection for the cigars.

The superior performance of the PAS-PDMS composite can be attributed to its unique structural design and material composition. The hierarchical water release mechanism and skin-like structural design enable precise and responsive humidity control. This ensures that the cigars are stored under optimal conditions, which is critical for preserving their quality and enhancing the smoking experience. Furthermore, the long-term stability of the PAS-PDMS composite in maintaining the desired humidity levels indicates its potential for practical applications in cigar storage and other environments requiring precise humidity control. The ability to maintain stable humidity levels over extended periods without significant performance degradation highlights the durability and effectiveness of the composite material.

### 3. Conclusion

This study introduces a novel PAS-PDMS composite hydrogel designed for microenvironmental humidity regulation, specifically applied to cigar storage. The composite exhibits remarkable mechanical and humidity control properties, providing a robust solution for maintaining optimal storage conditions. The integration of high-strength PDMS elastomer significantly enhances the structural network strength and mechanical properties of the PAS-PDMS composite. Rheological tests confirm that the composite maintains stable internal network strength and exhibits high storage modulus under strain, indicating its resilience under mechanical stress. The composite's superior mechanical performance ensures its durability and reliability in practical applications, particularly during the transportation and handling of cigars. Comprehensive analyses of the water migration and evolution mechanisms reveal that the PAS-PDMS composite systematically releases water molecules, allowing for stable and intelligent humidity regulation. The thermogravimetry-infrared analysis and low-field NMR tests demonstrate the composite's ability to maintain a controlled release of water, ensuring optimal humidity levels within a specified range. This unique hierarchical water release mechanism, coupled with the skin-like structural design, facilitates efficient humidity control even under extreme environmental conditions. Humidity control performance tests further validate the efficacy of the PAS-PDMS composite. The material consistently maintains effective humidity control across diverse environments, outperforming commercially available hydrogel-based moisturizing materials. The composite swiftly adjusts to changing humidity levels, maintaining the microenvironment within the optimal range for cigar storage and providing long-term stability for up to 20 days. This superior performance underscores the composite's potential for practical applications requiring precise humidity regulation. Therefore, the PAS-PDMS composite offers a robust,

durable, and efficient solution for humidity regulation, particularly in the context of cigar storage. Its advanced mechanical properties and intelligent humidity control capabilities make it a promising candidate for a wide range of applications where maintaining optimal humidity is critical.

## 4. Experimental section

### 4.1. Materials

Acrylamide (AM, analytical pure), produced by Chengdu Huaxia Reagent Factory; acetone glycerol (Sol, analytical pure), produced by Chengdu Kelong Chemicals Co., Ltd.; *N,N*-methylene bisacrylamide (MBA, analytical pure), produced by Admas-beta; acrylic acid (AA, analytical pure), produced by Chengdu Huaxia Reagent Factory; 2-hydroxy-2-methylpropanone (1173, analytical pure), produced by Admas-beta; deionized water, self-made; polydimethylsiloxane (PDMS, analytical pure), produced by Admas-beta; octamethylcyclotetrasiloxane (D4, analytical pure), produced by Admas-beta, 3-(trimethoxysilyl) propyl methacrylate (TMSPMA, analytical pure), produced by Admas-beta.

### 4.2. The preparation process of PAS-PDMS composite

(1) Preparation of PDMS elastomer: first, the PDMS elastomer was prepared by copolymerization. 10 g of PDMS was mixed with 0.5 g of D4 as a crosslinking agent. The mixture was thoroughly blended for 20 minutes, then poured into a rectangular mold and cured in a constant temperature drying oven at 60 °C for 1 hour to achieve complete curing and crosslinking. (2) Preparation of PAS hydrogel precursor solution: to prepare the PAS hydrogel precursor, 25 g of deionized water was mixed with 15 g of AM, and the mixture was stirred gently for 5 minutes until AM was fully dissolved. Next, 10 mg of MBA and 3 g of Gly were added sequentially, and stirring continued until a uniform solution was obtained. This solution was then transferred to a single-neck flask and purged with nitrogen to remove dissolved oxygen. (3) Preparation of PAS-PDMS composite: after deoxidizing the precursor solution, it was transferred to a beaker where 100  $\mu$ L of 3-(trimethoxysilyl)propyl methacrylate was added. The pH of the solution was adjusted to 4–5 using acrylic acid to promote the dissolution of the silane coupling agent. The treated precursor solution was then carefully poured into the PDMS elastomer mold, and 50  $\mu$ L of 2-hydroxy-2-methylpropiophenone was added. The system was gelled under ultraviolet irradiation from a high-pressure mercury lamp, resulting in the formation of the PAS-PDMS composite.

### 4.3. SEM test method

Characterize the micromorphology of PAS-PDMS composite by Carl Zeiss EV0-18 scanning electron microscope and X-MAX50MM2 energy dispersive spectrometer (EDS). After the material was pre-freeze-dried, its cross section was observed by a liquid nitrogen quenching section. The voltage during the test is 20 kV.



#### 4.4. Super depth of field optical microscope characterization (DOF) test method

The macro morphology of the hydrogel was characterized by DOF, and the PAS-PDM hydrogel was cut into a cube (1 cm × 1 cm × 1 cm), and the macro morphology of the hydrogel was characterized by four different magnifications of 20×, 30×, 50×, and 100×.

#### 4.5. FTIR infrared spectroscopy test

The molecular structure of the PAS-PDMS composite was characterized by the VERTEX 70 Fourier Transform Infrared Spectrometer (USA). The test wavelength is 400–4000 cm<sup>−1</sup>, and the test is carried out in ATR total reflection mode. Each sample is tested 3 times.

#### 4.6. UV test method

The transmittance of hydrogel was tested by the Lambda950 ultraviolet spectrophotometer (USA). The test wavelength is 400–800 nm.

#### 4.7. Mechanical properties tests

Mechanical behaviors of hydrogels were characterized by an Instron 3367 universal tensile testing machine (USA). Typical stress–strain curves were obtained by stretching samples at a rate of 100 mm min<sup>−1</sup> until fracture. The nominal fracture stress, fracture strain, elastic modulus (Young's modulus,  $E1$ ), and toughness were calculated from the stress–strain curves. True stress–strain curves were transformed through the relationship between true stress and nominal stress. True modulus and tensile strength were acquired from the true stress–strain curves. All stresses and moduli were nominal stress and nominal modulus if not otherwise indicated. To analyze the multiscale mechanics of hydrogels during stretching, cyclic tensile loading–unloading tests with different maximum strains ( $\epsilon_{\max}$ ) were conducted. To evaluate the rate dependence of modulus, samples were stretched to fracture at different rates. To investigate fatigue resistance and self-recovery properties of the hydrogel under stretching, sequential cyclic tensile loading–unloading tests and intermittent cyclic tensile loading–unloading tests were performed, respectively. Specimens were prepared as a dumbbell shape with a gauge length of 20 mm, a width of 4 mm, and a thickness of 0.8–2 mm. To investigate the fatigue resistance of the hydrogel under compression, sequential cyclic compression loading–unloading tests were performed. Specimens were prepared as a cylinders with a diameter of 10 mm and a height of 12 mm. To minimize dehydration during the cyclic test, the hydrogel samples were sealed by a homemade polymethyl methacrylate chamber. Water droplets were sprayed on the inner surface of the chamber to maintain the humidity. All the samples were weighed before and after the test, and the weight loss didn't exceed 5%.

#### 4.8. Water retention test method

The PAS-PDMS composite was cut into a 4 cm × 2 cm rectangular sample piece with a thickness of 1 mm through a cutter, and then the sample was placed in a constant temperature drying oven with a humidity of 65% RH and a set temperature of 30 °C. Test the weight every 3 h and record it. Set three parallel samples in the same group.

#### 4.9. Dynamic moisture adsorption test

The water absorption/release capacity and micro-release kinetics of the hydrogel were tested by the dynamic water vapor adsorption apparatus. The humidity gradient was set at 15%/45 min, the temperature was 25 °C, and the mass change rate was 0.008%.

#### 4.10. Thermodynamic parameter test

The thermodynamic parameters and free water crystallization peak of the water in the hydrogel were measured by a differential scanning calorimeter. The heating rate was 10 °C min<sup>−1</sup>.

#### 4.11. Low-field nuclear magnetic resonance test

The binding and release kinetics of water molecules in the hydrogel were characterized by low-field NMR, and the mode was set as T2 relaxation.

#### 4.12. Moisture-regulating performance test

The PAS-PDMS composite was placed in the cigar box, and monitored the humidity change of the microenvironment through the temperature and humidity meter. The whole test process was in the constant temperature and humidity box to maintain the constant temperature and humidity of the external environment.

### Data availability

The data that support the findings of this study are available within this article.

### Author contributions

Xiaoying Ji: conceptualization, methodology, resources, visualization. Xiaopeng Li: conceptualization, methodology. Juan Liu: methodology, investigation. Di Wu: investigation, formal analysis, writing—original draft preparation. Qianqian Liang: investigation, methodology. Beibei Zhu: investigation, resources. Wanjiao Fang: resources, formal analysis. Shirui Qiu: resources, visualization. Qianying Zhang: writing—review and editing, supervision, funding acquisition. Dongliang Li: supervision, project administration, funding acquisition. Lijuan Zhao: supervision, project administration, funding acquisition. Yi Wang: writing—review and editing, supervision, project administration.



## Conflicts of interest

The authors declare no conflict of interest.

## Acknowledgements

China Tobacco Sichuan Industrial Co., Ltd. (No. cl202103) is deeply appreciated for providing financial support in this work.

## References

- 1 R. E. Malone, The Tobacco Industry, 2020: A Snapshot, *Tob. Control*, 2020, **29**, e1–e3.
- 2 J. Ai, M. Hassink, K. M. Taylor, P. Kuklenyik, L. Valentin-Blasini and C. Watson, Tobacco-Specific Nitrosamines in Current Commercial Large Cigars, Cigarillos, and Little Cigars, *Chem. Res. Toxicol.*, 2024, **37**, 220–226.
- 3 S. D. Kowitt, S. A. Clark, K. L. Jarman, J. Cornacchione Ross, L. M. Ranney, P. Sheeran, J. F. Thrasher, C. Enyioha and A. O. Goldstein, Improving Point-of-Sale Warnings for Single Cigars: Implications for Premium Cigars, *Nicotine Tob. Res.*, 2023, **25**, S76–S80.
- 4 T. Zhao, G. Wang, D. Hao, L. Chen, K. Liu and M. Liu, Macroscopic Layered Organogel–Hydrogel Hybrids with Controllable Wetting and Swelling Performance, *Adv. Funct. Mater.*, 2018, **28**, 1800793.
- 5 Q. Ma, L. Wang, G. Xu, J. Li, M. Wang and C. Jiang, A novel low-voltage responsive NIPAAm/CNTs/Fe(phen)<sub>3</sub> double network shape-changing hydrogel with a balance between mechanical properties and deformation ability, *Polym. Test.*, 2023, **129**, 108277.
- 6 H.-Y. Wang, H.-D. Wang and Y.-Q. Zhang, A mechanically robust PVA-xylosylated sericin composite hydrogel membrane with enhanced biocompatibility by unidirectional dehydration through nanopore, *Polym. Test.*, 2023, **124**, 108062.
- 7 H. Lv, R. Xu, X. Xie, Q. Liang, W. Yuan, Y. Xia, *et al.*, Injectable, degradable, and mechanically adaptive hydrogel induced by L-serine and allyl-functionalized chitosan with platelet-rich plasma for treating intrauterine adhesions, *Acta Biomater.*, 2024, **184**, 144–155.
- 8 X. P. Morelle, W. R. Illeperuma, K. Tian, R. Bai, Z. Suo and J. J. Vlassak, Highly Stretchable and Tough Hydrogels below Water Freezing Temperature, *Adv. Mater.*, 2018, **30**, 1801541.
- 9 X. Xie, X. Ao, R. Xu, H. Lv, S. Tan, J. Wu, *et al.*, Injectable, stable, and biodegradable hydrogel with platelet-rich plasma induced by L-serine and sodium alginate for effective treatment of intrauterine adhesions, *Int. J. Biol. Macromol.*, 2024, **270**, 132363.
- 10 Y. Wang, P. Pan, H. Liang, J. Zhou, C. Guo, L. Zhao, *et al.*, Hemostatic Tranexamic Acid-Induced Fast Gelation and Mechanical Reinforcement of Polydimethylacrylamide/Carboxymethyl Chitosan Hydrogel for Hemostasis and Wound Healing, *Biomacromolecules*, 2024, **25**(2), 819–828.
- 11 Z. Wang, J. Chen, Y. Cong, H. Zhang, T. Xu, L. Nie and J. Fu, Ultrastretchable Strain Sensors and Arrays with High Sensitivity and Linearity Based on Super Tough Conductive Hydrogels, *Chem. Mater.*, 2018, **30**, 8062–8069.
- 12 L. Wang, G. Gao, Y. Zhou, T. Xu, J. Chen, R. Wang, R. Zhang and J. Fu, Tough, Adhesive, Self-Healable, and Transparent Ionically Conductive Zwitterionic Nanocomposite Hydrogels as Skin Strain Sensors, *ACS Appl. Mater. Interfaces*, 2019, **11**, 3506–3515.
- 13 S. Li, H. Pan, Y. Wang and J. Sun, Polyelectrolyte Complex-Based Self-Healing, Fatigue-Resistant and Anti-Freezing Hydrogels as Highly Sensitive Ionic Skins, *J. Mater. Chem. A*, 2020, **8**, 3667–3675.
- 14 J. Qu, X. Zhao, Y. Liang, T. Zhang, P. X. Ma and B. Guo, Antibacterial Adhesive Injectable Hydrogels with Rapid Self-Healing, Extensibility and Compressibility as Wound Dressing for Joints Skin Wound Healing, *Biomaterials*, 2018, **183**, 185–199.
- 15 H. Chen, F. Yang, Q. Chen and J. Zheng, A Novel Design of Multi-Mechanoresponsive and Mechanically Strong Hydrogels, *Adv. Mater.*, 2017, **29**, 1606900.
- 16 B. Hu, M. Gao, K. O. Boakye-Yiadom, W. Ho, W. Yu, X. Xu and X.-Q. Zhang, An Intrinsically Bioactive Hydrogel with On-Demand Drug Release Behaviors for Diabetic Wound Healing, *Bioact. Mater.*, 2021, **6**, 4592–4606.
- 17 Q. Li, Y. Zhang, X. Huang, D. Yang, L. Weng, C. Ou, X. Song and X. Dong, An NIR-II Light Responsive Antibacterial Gelation for Repetitious Photothermal/Thermodynamic Synergistic Therapy, *Chem. Eng. J.*, 2021, **407**, 127200.
- 18 X. Cui, B. G. Soliman, C. R. Alcala-Orozco, J. Li, M. A. M. Vis, M. Santos, S. G. Wise, R. Levato, J. Malda, T. B. F. Woodfield, *et al.*, Rapid Photocrosslinking of Silk Hydrogels with High Cell Density and Enhanced Shape Fidelity, *Adv. Healthcare Mater.*, 2020, **9**, 1901667.
- 19 S. Yan, W. Wang, X. Li, J. Ren, W. Yun, K. Zhang, G. Li and J. Yin, Preparation of Mussel-Inspired Injectable Hydrogels Based on Dual-Functionalized Alginate with Improved Adhesive, Self-Healing, and Mechanical Properties, *J. Mater. Chem. B*, 2018, **6**, 6377–6390.
- 20 Y. Fan, M. Luchow, Y. Zhang, J. Lin, L. Fortuin, S. Mohanty, A. Brauner and M. Malkoch, Nanogel Encapsulated Hydrogels As Advanced Wound Dressings for the Controlled Delivery of Antibiotics, *Adv. Funct. Mater.*, 2021, **31**, 2006453.
- 21 R. Fu, L. Tu, Y. Zhou, L. Fan, F. Zhang, Z. Wang, J. Xing, D. Chen, C. Deng, G. Tan, *et al.*, A Tough and Self-Powered Hydrogel for Artificial Skin, *Chem. Mater.*, 2019, **31**, 9850–9860.
- 22 X. Yang, Z. Fan, H. Zhang, W. Xu and Z. Wu, Energy Harvest from Contaminants via Coupled Redox Fuel Cells, *Energy Procedia*, 2017, **105**, 1852–1857.
- 23 S. Lin, J. Liu, X. Liu and X. Zhao, Muscle-like Fatigue-Resistant Hydrogels by Mechanical Training, *Proc. Natl. Acad. Sci. U.S.A.*, 2019, **116**, 10244–10249.
- 24 H. Chen, F. Yang, Q. Chen and J. Zheng, A Novel Design of Multi-Mechanoresponsive and Mechanically Strong Hydrogels, *Adv. Mater.*, 2017, **29**, 1606900.
- 25 X. Wang, G. Chen, J. Tian and X. Wan, Chitin/Ca Solvent-Based Conductive and Stretchable Organohydrogel with





- Anti-Freezing and Anti-Drying, *Int. J. Biol. Macromol.*, 2022, **207**, 484–492.
- 26 G. Cai, J. Wang, K. Qian, J. Chen, S. Li and P. S. Lee, Extremely Stretchable Strain Sensors Based on Conductive Self-Healing Dynamic Cross-Links Hydrogels for Human-Motion Detection, *Advanced Science*, 2017, **4**, 1600190.
- 27 H. Lu, W. Shi, J. H. Zhang, A. C. Chen, W. Guan, C. Lei, J. R. Greer, S. V. Boriskina and G. Yu, Tailoring the Desorption Behavior of Hygroscopic Gels for Atmospheric Water Harvesting in Arid Climates, *Adv. Mater.*, 2022, **34**, 2205344.
- 28 J. Löfgren and F. Lohmander, Silicone Breast Implants and Disease—Many Questions Unanswered, *JAMA Netw. Open*, 2021, **4**, 2128947.
- 29 K. H. Bae, L.-S. Wang and M. Kurisawa, Injectable Biodegradable Hydrogels: Progress and Challenges, *J. Mater. Chem. B*, 2013, **1**, 5371.
- 30 Y. Huang, S. Qian, J. Zhou, W. Chen, T. Liu, S. Yang, *et al.*, Achieving Swollen yet Strengthened Hydrogels by Reorganizing Multiphase Network, *Adv. Funct. Mater.*, 2023, **33**, 2213549.

